

LIQUID ROCKET COMBUSTOR COMPUTER CODE DEVELOPMENT*

P. Y. Liang

Rockwell International/Rocketdyne Division
Canoga Park, California

Abstract

This paper highlights the Advanced Rocket Injector/Combustor Code (ARICC) that has been developed at Rocketdyne to model the complete chemical/fluid/thermal processes occurring inside rocket combustion chambers. The code, derived from the CONCHAS-SPRAY code originally developed at Los Alamos National Laboratory (Ref. 1) incorporates powerful features such as the ability to model complex injector combustion chamber geometries, Lagrangian tracking of droplets, full chemical equilibrium and kinetic reactions for multiple species, a fractional volume of fluid (VOF) description of liquid jet injection in addition to the gaseous phase fluid dynamics, and turbulent mass, energy, and momentum transport. Atomization and droplet dynamic models from earlier generation codes are transplanted into the present code. Currently, ARICC is specialized for liquid oxygen/hydrogen propellants, although other fuel/oxidizer pairs can be easily substituted. ARICC is a two-dimensional/axisymmetric real-time transient code, and effort on developing a three-dimensional counterpart is underway.

Introduction

Combustion processes occurring in a fluid medium are probably among the most complex of all flow phenomena. The complexity stems from two primary reasons. Firstly, the so-called "combustion" process actually encompasses many physical processes of different types,

*Sponsored by NASA under Contract NAS8-34928.

different natures, different temporal and spatial scales, and different degrees of being describable by deterministic models. Secondly, all of these processes are usually strongly coupled together, making it difficult to reduce the problem down to its individual component processes. Any attempt to numerically model such complex combustion phenomena would need to make careful distinction between those processes that can be considered as the primary driving ones, and hence, should be modeled as vigorously as possible, and those that can be considered secondary and are included only for their usefulness in "interpreting" the situation into the desired results. Such decisions are often as important as the quality of the mathematical models themselves.

Inside a liquid rocket engine, the process usually starts with the injection of fuel and oxidizer into the combustion chamber in both liquid and gaseous states under high pressure and at greatly different velocities so as to encourage rapid atomization of the liquid component. The flow created by such injection is highly turbulent and rotational. Furthermore, in the case of liquid oxygen/hydrogen engines, the propellants are at temperature extremes ranging from cryogenic (70 K) to superhot (3000+ K). Thus, even in the precombustion state the flow is fully elliptic and composed of multiple species with real gas/liquid properties. The inception of combustion magnifies the local temperature, pressure, and species concentration gradients, and adds one more time scale to those of the bulk flow transience and of the turbulence. In light of these circumstances, a list of requirements deemed necessary for the numerical modeling of the combustion process has been generated and are listed in Table 1.

The ARICC code represents an attempt to build a modular model to describe the complete combustion process inside a liquid rocket engine using state-of-the-art finite difference techniques. It is an advancement over earlier-generation performance codes, many of which are used as industrial standards, that frequently describe one aspect of the combustion

Table 1. Code Features Required for Liquid Rocket Engine Modeling

NECESSARY FEATURES	FEATURES INCORPORATED INTO ARICC
<ul style="list-style-type: none"> • VISCOUS ELLIPTIC FLOW • FULL CHEMISTRY • LIQUID JET INJECTION/ 2 PHASE FLOW • DROPLET DYNAMICS • ATOMIZATION • FINE RESOLUTION IN CRITICAL AREAS 	<ul style="list-style-type: none"> • FULL NAVIER-STOKES EQN. + SGS TURBULENCE MODEL, ALL FLOW SPEEDS. • MULTIPLE SPECIES KINETIC AND EQUILIBRIUM REACTIONS • VOF TWO-PHASE, FREE SURFACE DESCRIPTION • MONTE CARLO SCHEME/LAGRANGIAN DROPLET TRACKING, DROPLET HEATUP AND VAPORIZATION • CICM ATOMIZATION MODEL • ARBITRARY GRID WITH CLUSTERING.

process in great detail (e.g., chemistry) but make gross assumptions about the other aspects (e.g., neglecting flow recirculation by using the stream tube method). These codes (Ref. 2-6) with their primary limitations are listed in Table 2. However, they all contain valuable experience and empirical models that have and will continue to be assimilated into the ARICC code.

Table 2. Earlier-Generation Rocket Combustion Codes

CODE NAME	PRIMARY FUNCTIONS	MAJOR LIMITATIONS
CICM ²	STEADY-STATE ROCKET COMBUSTION OF H ₂ /LOX FOR COAXIAL INJECTION	STREAM TUBE FLUID DYNAMICS. ATOMIZATION CORRELATIONS FROM J-2 ENGINE
TRANS78 ³	MULTIPURPOSE CHEMISTRY CODE FOR ROCKET PERFORMANCE, DETONATION, CONSTANT P OR CONSTANT V COMBUSTION ETC.	1D EQUILIBRIUM ISENTROPIC. NO SPATIAL RESOLUTION OR FLOW DYNAMICS
SDER ⁴	STEADY-STATE 1D FLUID DYNAMICS WITH 3D DROPLET DYNAMICS FOR IMPINGING TYPE ELEMENTS. LIQUID/GAS, SUB. AND SUPER-CRITICAL VAPORIZATION OF DROPLETS	DROPLET CORRELATIONS DEVELOPED FROM COLD FLOW. STREAM TUBE FLUID DYNAMICS
TPP ⁵	TIME-DEPENDENT PROGRAM FOR SMALL PULSED TYPE ENGINES WITH HYPERGOLIC PROPELLANTS. 3D DROPLET DYNAMICS.	1D FLUID DYNAMICS. IMPINGING LIQUID-LIQUID ELEMENTS ONLY. SUBCRITICAL DROPLETS
GKAP ⁶	STEADY-STATE CHEMICALLY REACTING GAS MIXTURES OF UP TO 150 SPECIES AND 70 NONEQUILIBRIUM REACTIONS.	1D FLOW. ADIABATIC COMBUSTION CHAMBER. NO DROPLETS.

Process of Code Development

The process of code development consists of four steps: (1) identify the critical processes; (2) determine which of these processes can be described vigorously and which should be modeled empirically, and devise mathematical expressions for each category; (3) translate these expressions into numerical formulations and assemble a logical algorithm for evaluating them and displaying the results; and (4) design steps for verification of the model components and for "anchoring" or fine-tuning of the empirical model constants.

The above process is depicted in Fig. 1. As a result of the initial scrutiny in step one, several assertions can be made concerning liquid rocket combustion. First, of the two primary transport processes of diffusion and convection (radiation is not important at these temperatures), the former controls the transfer of species with respect to each other while the latter controls the bulk transfer of mass, momentum, and energy. As the liquid oxygen/hydrogen reactions are relatively fast, the steady-state flame is thus diffusion controlled and can be described sufficiently with equilibrium reactions. Viscosity (diffusive transfer

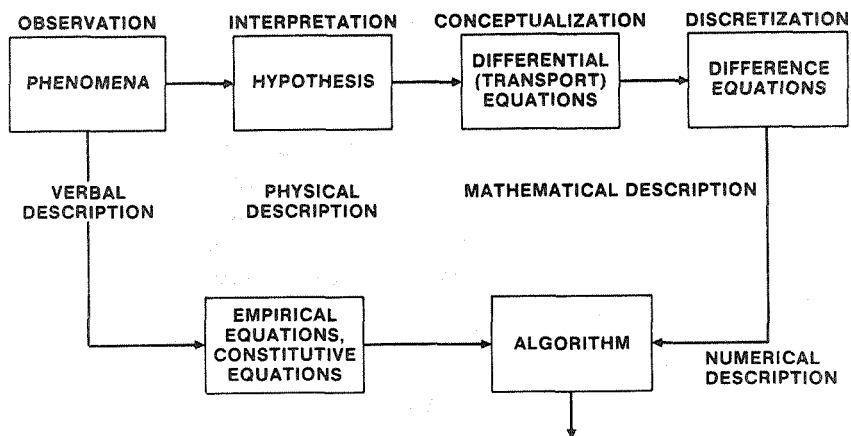


Fig. 1. Steps in Formulation of a Computer Model

of momentum) is important only in stagnant zones of the combustion chamber where recirculation controls wall heat transfer, and indirectly through the turbulence scale which affects the species diffusion and atomization processes. Second, the overall performance of the rocket engine is strongly dependent on the effectiveness of the atomization process. Unvaporized and hence uncombusted droplets are the greatest cause of loss of engine efficiency. Third, while the steady-state flame is adequately described by a diffusion-controlled equilibrium flame model, the ignition and flame holding mechanisms and wall-streaking phenomenon of concern can only be understood with detailed consideration to the local geometry and flow patterns and transient heat transfer processes. The life and durability of the engine depends largely on these last mechanisms.

In other words, an adequate numerical model must have the capability to fully describe the following types of phenomena: viscous flow as described by the full Navier-Stokes equations with turbulence modeling; multiple species chemical kinetics, liquid jet injection, atomization, and subsequent vaporization and transport of the droplets; and fine grid resolution near boundaries and corners of particular interest. All of these capabilities have been built into ARICC. The type of mathematical model used for each phenomena is listed in Table 3.

Before a more detailed description is given of the code, a comment about the code's verification is in order. The basic fluid dynamics, which forms the basis of the solution scheme, will and is being checked out with experimental laser velocimetry measurements done on a low pressure cold flow test chamber under the current contract, and the final results will be reported in a future writeup. Optical Schlieren and infrared data obtained in the same tests also provide a qualitative means of verifying the overall temperature profiles. Far more critical however are the verification needs pertaining to the empirical models, where the greatest uncertainty lies and where the greatest variation from problem to problem still exists in the form

Table 3. Mathematical Formulation Used for Various Physical Processes

I. FLUID THERMODYNAMICS	
MASS CONSERVATION (CONTINUITY)	PD
MOMENTUM CONSERVATION (NAVIER-STOKES)	PD
ENERGY CONSERVATION	PD
II. PHYSICAL MODELS	
EQN. OF STATE (CONSTITUTIVE)	AL/TA
TURBULENCE	AL/PD
CHEMISTRY	
RATE EQUATIONS	AL
EQUILIBRIUM EQUATIONS	AL/TA
RADIATION	PD
III. DROPLET DYNAMICS	
DISCRETE FORMULATION	OD
CONTINUUM FORMULATION	OD
	PD
<u>TYPE OF GOVERNING EQN.</u>	
PD	= PARTIAL DIFFERENTIAL
AL	= ALGEBRAIC
TA	= TABULAR
OD	= ORDINARY DIFFERENTIAL

of arbitrary coefficients. Replacing these coefficients with universal constants or expressions is a task of utmost concern. This applies to the turbulence model, supercritical droplet properties, the atomization model, as well as the droplet heatup and vaporization models. Few correlations are available and measurements are difficult to make and hard to come by, especially in the area of droplet dynamics. Finally, the choice of chemical equations, species, and rate or equilibrium constants to describe the chemical processes also represents a major area of uncertainty. In the case of oxygen/hydrogen kinetics, the role of the third body reactions is largely undetermined. An initial one-dimensional test case using the ARICC code however does indicate that the resulting temperature profile inside a premixed combustor tube is strongly influenced by the omission of certain third-body reactions. Much study is still required before any conclusion can be made.

Code Description

Code Organization

Figure 2 shows the organization of ARICC, which is typical of a full-fledged combustion code. As previously stated solution of the fluid dynamic governing equations of mass, momentum, and energy with attending boundary conditions form the core of the numerical algorithm. On top of that, the empirical models describing the gas or liquid properties (enthalpy tables, vapor pressure curve fits, etc.), the chemical reactions, the atomization and droplet heatup and evaporation processes, and the turbulence model are called

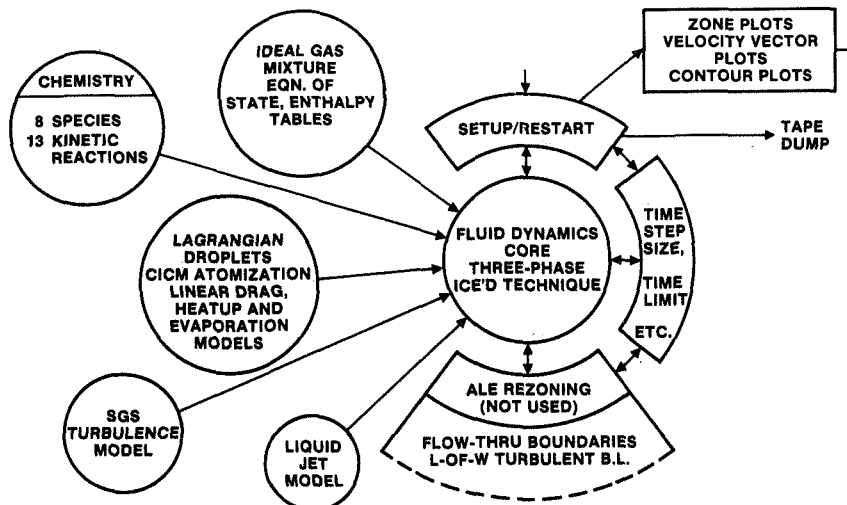


Fig. 2. Current ARICC Code Organization

as subroutines as and when they are required. To make an operationally useful code, however, the code must be given a flexible input/output capability for grid generation, field initialization, and graphical and tabular display of outputs. All these functions are in turn controlled by a master main program which also takes the responsibility of ensuring stability through time-step size control and various artificial numerical smoothing schemes. Figure 3 is a simplified flow chart of ARICC.

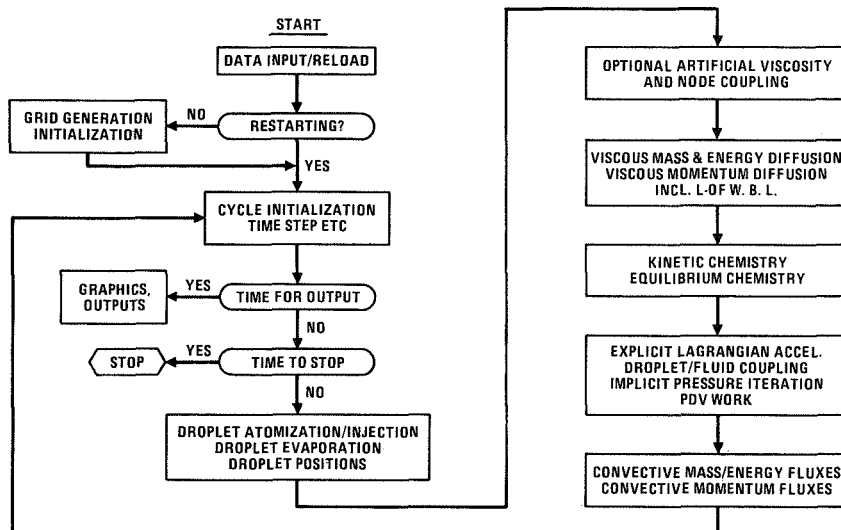
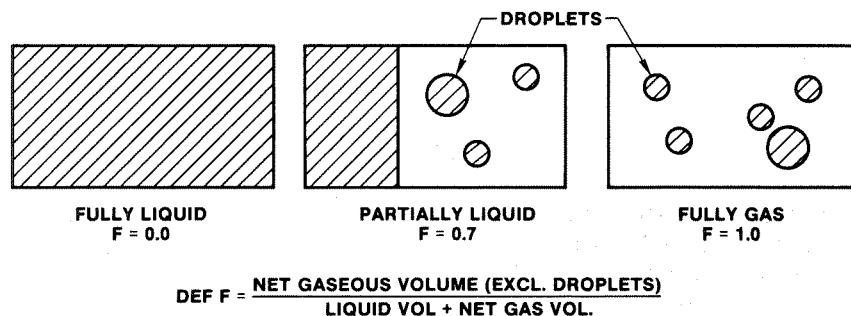


Fig. 3. Simplified Flow Chart ARICC Code

Basic Solution Algorithm

The basic Implicit Continuous Eulerian with Arbitrary Lagrangian-Eulerian (ICE'd-ALE) mesh treatment solution technique used in ARICC has been described in detail in Ref. 1 and will not be repeated here. The major complication involved in the ARICC code is the need to handle both compressible gases and incompressible liquid within the numerical framework. To do this, cells that contain liquid must first of all be distinguished from cells that do not. To this end, the Fractional Volume of Fluid method of description has been adopted from the free surface flow SOLA-VOF program (Ref. 7). A cell flag variable (F) is used to represent the fraction of the volume of a cell that is occupied by compressible gases. Thus, three different kinds of active cells are possible (Fig. 4). Cells that are totally or partially gaseous (with F values greater than 0 and less than or equal to 1) will be treated as a "normal" cell using the standard ICE'd pressure iteration scheme. However, the cell volume used in the calculation will be that of the effective gaseous volume equal to F times the total active cell volume. Cells with flag value equal to

• ACTIVE CELLS DISTINGUISHED BY THEIR FLAG VALUES:



- DROPLETS MAY EXIST IN CELLS WITH $F > 0.0$
- SINGLE-VALUED THERMODYNAMIC PROPERTIES FOR ALL CELLS
- PRESSURE IN FULLY LIQUID CELLS DETERMINED BY PRESSURE ITERATION SCHEME FOR INCOMPRESSIBLE FLUID

Fig. 4. Different Types of Active Cells in Two-Phase ARICC

0 are fully liquid cells, and while they are treated the same way in the rest of the program, in the pressure iteration step these cells are given a "pseudo-incompressible" treatment by using a pressure iteration scheme that tries to enforce a conservation of the fluid volume, and hence density (Ref. 8). No equation of state relation is applied to the liquid portions and a constant density (as well as temperature) is simply assumed. Chemical reactions are permitted only inside the gaseous phase and no direct mass or heat transfer takes place across the gas/liquid interface. Thus, other than for the fluid dynamical interactions, the only path by which the liquid affects the gaseous mixture is by first turning into droplets and evaporating. The atomization model is described below.

Since the main reason for inclusion of the liquid phase description is for modeling of the liquid jet column coming in through the coaxial injector of a rocket engine, the bulk of the liquid is currently assumed to be always around the central axis of the model. This simplifies the determination of the orientation of the liquid-gas interface necessary for the

calculation of the flux of liquid from one partially liquid cell to the next, and also simplifies the graphics scheme for plotting the interface. A generalization to accommodate the most arbitrary liquid-gas combination can be readily made.

Atomization Model

At designated intervals, numerical droplet groups representing a number of particles of the same properties are created from the cells that contain a liquid-gas boundary. The atomization model consists of calculation of the stripping rate and the mean drop size (and possibly a statistical distribution function of the drop sizes) from the local fluid dynamic properties. Currently, the model used in ARICC is that taken from the CICM program (Ref. 2). The expressions are as follows:

$$\text{Mean Stripping Rate } M_A = C_A \left[\frac{\mu_j (\rho_g U_r)^2}{\sigma_j / \rho_j} \right]^{1/3} \pi D_j (\Delta Z)$$

$$\text{Mean Drop Size } \bar{D}_j = B_A \left[\frac{\mu_j (\sigma_j / \rho_j)^{1/2}}{\rho_g U_r^2} \right]^{2/3}$$

where

- C_A, B_A = empirical constants
- D_j = jet diameter
- U_r = gas velocity relative to liquid jet
- Z = axial location
- ρ_g, ρ_j = gas, jet density
- μ_j = jet viscosity
- σ_j = jet surface tension

At creation, the droplets are given a temperature and density equal to those of the liquid from which

they are created, and an appropriate amount of liquid is eliminated from the cell liquid volume. The reverse process of droplet "recondensation" into the liquid is also allowable, if the droplet velocity should lead it to head back toward a liquid surface. Also, the droplets are given an initial speed equal to that of the local liquid surface and a direction that randomly spans a 90-degree fan, ranging from being aligned with the liquid surface to being radially away. Obviously, these fine details of the model are somewhat arbitrary and can be changed as more experimental data becomes available.

Both because of the fact that the complete atomization process from liquid medium is being modeled and because of the substantial density and sizes of droplets dealt with in liquid rocket engines (up to 100 microns as compared with submicron droplets usually encountered in gas turbines), the droplets in ARICC are given a finite volume that would physically exclude gas and liquid from within the cell. Dynamically speaking, the "bouyancy" term is being included. Thus, the droplet volumes enter into the determination of the effective (gaseous) cell volume. This situation is also depicted in Fig. 4. However, a droplet can only be in one computational cell at any time, as its location is uniquely defined by a single set of coordinates. Currently, interaction among droplets (e.g., coagulation) and film formation along solid surfaces as the droplets hit the walls are not modeled.

This advanced description of the droplet spray plus the two-phase liquid jet description and the CICM atomization model make the ARICC code unique in its capability for modeling liquid rocket engines. The entire combustion process can now be analyzed, in whole rather than in parts. It combines the different branches of fluid dynamics, namely, two-phase flow, reactive flow, particulate flow, and compressible recirculating flow into a single transient finite difference model. The atomization process

that is so important to rocket engine performance can now be studied. Finally, the droplet finite volume displacement and recondensation features pave the way for simulation of droplet breakup and coagulation phenomena.

Oxygen/Hydrogen Chemistry Model

Although the primary reactions of the oxygen/hydrogen chemistry are well known, the secondary reactions, especially those involving third bodies, are much more difficult to pinpoint. Only equilibrium reactions are necessary for steady-state, strictly diffusion-control flames. But to simulate the transient processes of ignition and flame propagation, kinetic reactions must be used, otherwise it was found that the flame propagation speeds will be unrealistically large. In its present configuration, the chemistry model in ARICC consists of 13 kinetic reactions involving 8 chemical species, of which 9 are elementary reactions and 4 are third-body reactions. The elementary reactions are the same as those used by Westbrook (Ref. 9). These reactions are summarized in Table 4. The adequacy or redundancy of these reactions for various situations are still being investigated.

Boundary Conditions

To complete this brief description of ARICC, mention should also be made of the boundary conditions currently in effect. For the purpose of modeling coaxial injector combustion chambers, ARICC is run in its axisymmetric mode with specified inflow conditions. The exit plane, which in most cases is a sonic nozzle throat, is treated as a specified pressure boundary. Other outflow conditions such as a zero-velocity gradient or enforced sonic conditions can also be specified. On the solid walls or internal solid boundaries, the boundary layer is approximated with a law-of-the-wall treatment. Sometimes a simple no-slip boundary condition

Table 4. List of Hydrogen/Oxygen Kinetic Reactions Currently Used in ARICC

1. $H + O_2$	\rightleftharpoons	$O + OH$
2. $H_2 + O$	\rightleftharpoons	$H + OH$
3. $H_2O + O$	\rightleftharpoons	$OH + OH$
4. $H_2O + H$	\rightleftharpoons	$H_2 + OH$
5. $H_2O_2 + OH$	\rightleftharpoons	$H_2O + HO_2$
6. $HO_2 + H$	\rightleftharpoons	$2 OH$
7. $HO_2 + H$	\rightleftharpoons	$H_2 + O_2$
8. $H_2O_2 + O_2$	\rightleftharpoons	$2 HO_2$
9. $H_2O_2 + H$	\rightleftharpoons	$HO_2 + H_2$
THIRD BODY REACTIONS:		
10. $H + O_2 + H_2$	\rightleftharpoons	$HO_2 + H_2$
11. $H + 2O_2$	\rightleftharpoons	$HO_2 + O_2$
12. $H + O_2 + H_2O$	\rightleftharpoons	$HO_2 + H_2O$
13. $H_2O_2 + H_2O_2$	\rightleftharpoons	$2OH + H_2O_2$

is preferred in the case of complicated surface contours. Details of the law-of-the-wall treatment are also discussed in Ref. 1.

Examples

Several cases of test runs are presented here to illustrate the qualitative features of the ARICC code.

Propagation of Flame Front

Figure 5 shows the model of a typical coaxial injector and combustion chamber. To check the one-dimensional flame propagation speed, the chamber is sealed off and filled with a premixed oxygen/hydrogen gas of 1:1 mixture ratio at 2000 psi and 298 K. At time 0, the entire upper row of cells is injected with a sufficient amount of energy to ignite the mixture, and the plane flame "sheet" propagates downward. It is interesting to note that a pressure wave travels at shock speed ahead of the flame front, which travels at the much lower speed of heat wave or concentration wave propagation. The flame front

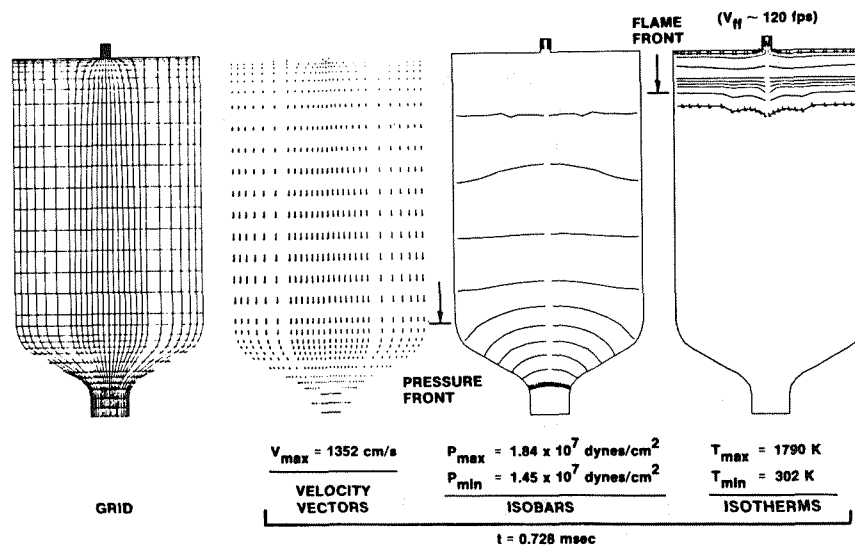
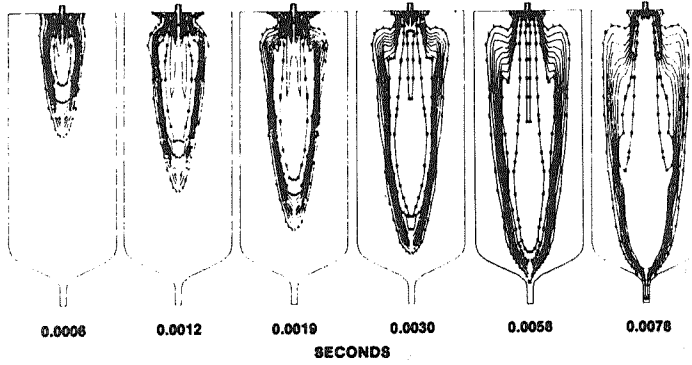


Fig. 5. Propagation of Plain Flame Front

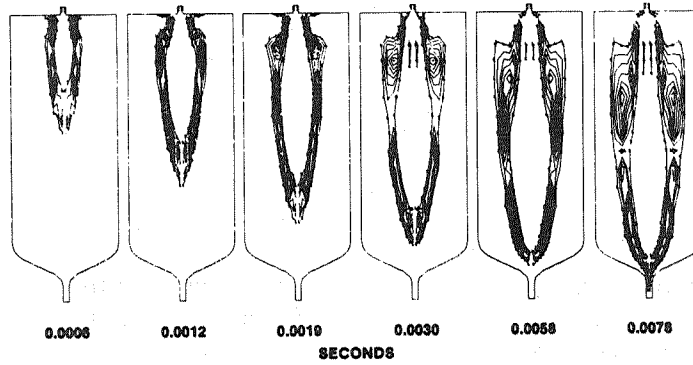
speed is estimated to be approximately 120 ft/sec, compared with the theoretical estimate (through SSME data correlation) of 114 ft/sec. Also at later times, it is noticeable that the planeness of flame front starts to deteriorate, partly because of the presence of the injector at the axis and partly because of the computational truncation errors toward the axis of symmetry.

Transient Ignition in Prefilled Chamber

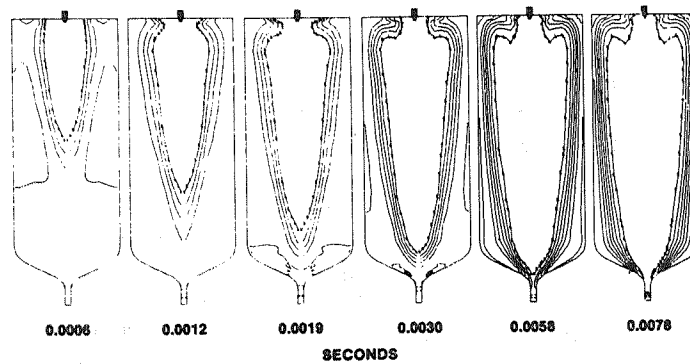
In the second example, a similar combustion chamber has been prefilled with pure oxygen gas at 15 psi at 298 K. At time zero, a coaxial stream of gaseous hydrogen and oxygen at a mixture ratio of 1 starts coming in through the injector. Near the injector entrance and slightly off the axis, a "spark" is ignited. The flow exits at the nozzle into atmospheric pressure. Figure 6 is a sequence of transient contour plots of water mass fractions, of hydrogen mass fractions, and of isotherms, and Fig. 7 is the velocity plot of the case early after startup showing the axisymmetric jet profile of the incoming hydrogen. The propagation of the major flame front, as diffused hydrogen reacts with the abundant oxygen, is evident. In this case, the



A. H_2O Mass Fraction



B. OH Mass Fraction



C. Density

Fig. 6. Transient Ignition in an Oxygen-Prefilled Chamber

VELOCITY VECTORS
EARLY AFTER STARTUP
T = 0.0006 SECONDS
MR = 1.0
 $V_{MAX} = 8.55 \times 10^4$ cm/sec
 $V_{zh,H_2} = 7.55 \times 10^4$ cm/sec
 $V_{zh,O_2} = 1.35 \times 10^4$ cm/sec

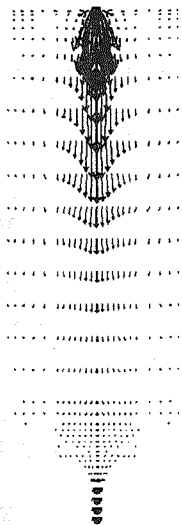


Fig. 7. Velocity Vector Plot of Incoming H_2/O_2 Coaxial Jet Stream

flame front is clearly defined by the sharp temperature gradients and the presence of combusted products, such as water, with relatively uniform conditions in the combusted region behind. In addition to the major flame front, however, a smaller secondary and more permanent flame is being established right at injector entrance. This is the steady-state flame that is of more ultimate interest. At $MR = 1$, it is a fuel-rich flame, and both its size and intensity is dwarfed by the transient flame front propagating outward into the prefilled chamber. Yet as the transient flame propagates outward, its speed slows down, and it takes a long time (more than 20 msec) for it to consume all the prefill oxygen and burn itself out. For this reason, another case is run in an attempt to simulate the steady state in a reasonably short time.

Steady-State Hydrogen/Oxygen Flame

In the third example, the same combustion chamber is now prefilled with the combustion products of the incoming hydrogen/oxygen stream at the estimated steady-state chamber pressure of 98 psi and temperature of 797 K. The gaseous coaxial streams, this time

at the mixture ratio of 0.5, again comes in from the top. After approximately 3 msec, the "steady state" is well established. The isotherms, the H₂O mass fraction contours, and the OH mass fraction contours are shown in Fig. 8. The presence of OH is probably the indicator of where the chemically active region is. In this case, however, difficulty has been experienced in maintaining the flame. As soon as the spark is turned off, the flame has a tendency to quench out. Indeed, in comparable experiments, sometimes, though not consistently, the same problem of flame ignition has been experienced. Thus, it appears that the problem is related to the details of the flame holding mechanism at the injector element tip, where the geometry is now only very coarsely modeled. A numerical model using

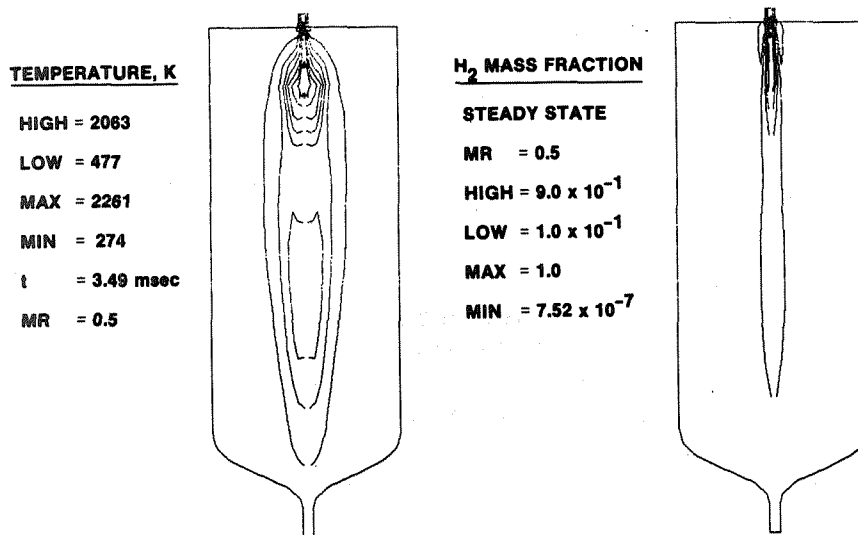


Fig. 8. Steady-State Combustion of Gaseous Oxygen/Hydrogen Flame

ARICC with very fine resolution around the injector should provide interesting insight into the exact nature of the flame holding mechanism there.

Liquid Jet Injection and Atomization

In the final example, the unique capability of ARICC to handle two-phase flow and the creation of droplets from a liquid jet is demonstrated. Instead of gaseous oxygen, a stream of liquid oxygen (density = 69.97 lb/ft³, temperature = 94.4 K) comes in through the center of the injector element. Gaseous hydrogen at atmospheric temperature comes in through the outer annulus at the high speed of 278 ft/sec (compared with 4.4 ft/sec for the oxygen) to achieve a mixture ratio of one. The chamber is prefilled with hydrogen at 100 psi and atmospheric temperature. Figure 9 is a sequence of plots showing the atomization process, and

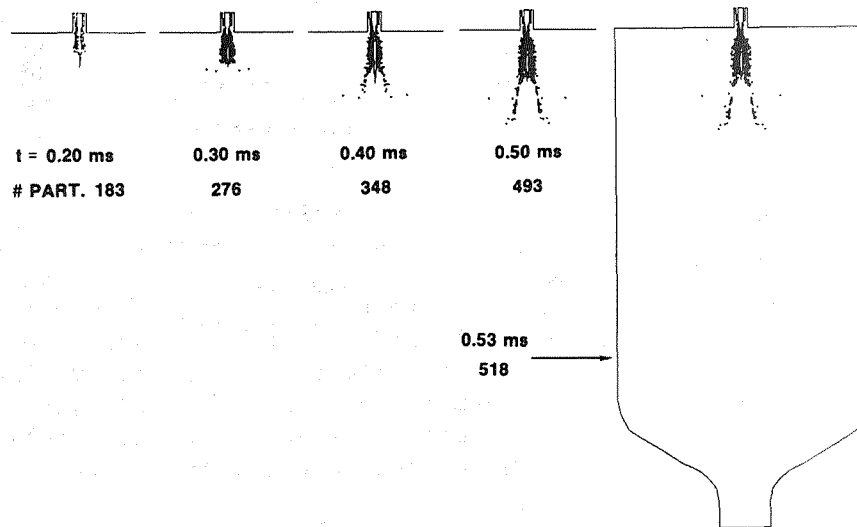


Fig. 9. Atomization Sequence of a Coaxial LOX Jet

Fig. 10 is a closeup view of the evolving shape of the liquid jet. At this range of relative velocities, droplets of the order of 10 microns are typically formed, mostly right in the recessed "cup" region shortly after injection. Note that the number of particles indicated in the figure are numerical droplet groups, with each group representing a certain number of actual physical particles depending on the local stripping rate at time of creation according to the

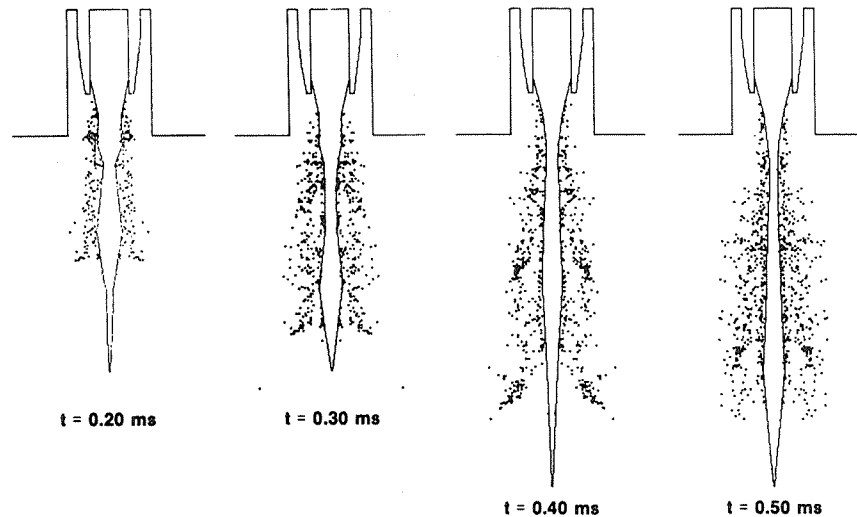


Fig. 10. Closeup Details of an Evolving Liquid (LOX) Jet

CICM atomization model. At the beginning of the run, the liquid jet column is given an arbitrary convenient shape (conforming to grid lines) with kinks on its surface. Toward the end of the run, at approximately 0.4 msec, it can be seen that the fluid dynamic forces have elongated the liquid column and smoothed out its surface. Though no experimental data are available now for a direct comparison, the simulated jet size and shape and the spray cone angle of the droplets (approximately 25 degrees) are all intuitively correct.

Conclusions and Recommendations

The ARICC code has shown that with present-day computers and numerical methodology, it is now possible to construct a complete model of the combustion process inside a liquid rocket engine. The development process points to many areas for further work, not the least of which is the need for experimental correlations to be fed into the many physical models that still need to be described empirically. Much specific measurements need to be done, using nonintrusive flow diagnostic techniques and spray measuring techniques, before the physical models can be confidently anchored and refined.

On the other hand, the availability of a tool like ARICC also opens up many potential applications. Already mentioned is the use of ARICC as a comprehensive simulator for injector/combustor hardware and other combustion devices. Secondly, ARICC can be used as an engine performance analyzer, especially when small but powerful dedicated computers are available. In this application, ARICC combines the diverse capability of and will eventually supercede the earlier generation codes stated previously (Ref. 2-6). The third and most promising area of application is ARICC as a research tool. While various physical models are now installed in ARICC, it can be turned around and used as a test bed for various upgraded models as new theories or data become available. Included in this category are areas for computational fluid dynamics research, such as turbulence models, algorithm efficiency improvements, and advanced graphics. Droplet dynamics research includes spray characteristics, droplet breakup/coagulation criteria, droplet deformation effects, atomization mechanism, and suspension flow or slurry flow. Thirdly, and most importantly, flame research using ARICC can be very fruitful in furthering understanding of diffusion flames, detonations, deflagrations, flame front propagation, ignition criteria, flame stability, and kinetic chemistry models. Finally, it should be remembered that ARICC is a two-dimensional/axisymmetric code. While already extremely valuable, most real-life hardware would require a fully three-dimensional model to study. Thus, the development of a three-dimensional counterpart to ARICC would be the logical next step to pursue.

Acknowledgement

The author wishes to acknowledge the following individuals at Rocketdyne for their continuing contributions to the development of ARICC: Mr. Steve Fisher, Dr. Mason Change, Dr. Robert Jensen, Mr. Raj Varma, and Mr. Paul Reiser for his programming expertise. Also acknowledged should be the authors of the CONCHAS-SPRAY code at Los Alamos National Laboratories.

References

1. Cloutman, L. D., J. K. Dukowicz, J. D. Ramshaw, and A. A. Amsden, CONCHAS-SPRAY: A Computer Code for Reactive Flows With Fuel Sprays, Los Alamos National Laboratories Report LA-9294-MS (1982).
2. Sutton, R. D., M. D. Schuman, and W. D. Chadwick, Operating Manual for Injection Combustion Model, Final Report, NAS8-29664 (1974).
3. Svehla, R., FORTTRAN IV Computer Program Calculation of Thermodynamic and Transport Properties of Complex Chemical Systems (TRANS 78 Program), NASA TND-7056 (1973).
4. Schuman, M. D., Standardized Distributed Energy Release Computer Program, Final Report Vol. I and II, AFRPL-TR-78-7 (1978).
5. Weber, W. T., et al., Transient Performance Programs, Vol. I and II, AFRPL-TR-80-22 (1980).
6. Nicholson, G. R. and D. E. Coats, Computer Program for the ANALYSIS of Chemically Reacting Gas Mixtures, Ultra Systems, Inc. (formerly Dynamic Sci.) Irvine, California (1973).
7. Nichols, B. D., C. W. Hirt, and R. S. Hotchkiss, SOLA-VOF: A Solution Algorithm for Transient Fluid Flow With Multiple Free Boundaries, Los Alamos National Laboratories, LA-8355 (1980).
8. Amsden, A. A., H. M. Ruppel, and C. W. Hirt, SALE: A Simplified ALE Computer Program for Fluid Flow at All Speeds, Los Alamos National Laboratories, LA-8095, pp 10-12 (1980).
9. Westbrook, C. K., "Oxidation Kinetics in Detonations," Comb. Sci. Tech., Vol 29 (1982).